BIOCHEMISTRY
including biophysical chemistry & molecular biology

Article

pubs.acs.org/biochemistry

Mutagenesis of a Conserved Glutamate Reveals the Contribution of Electrostatic Energy to Adenosylcobalamin Co−C Bond Homolysis in Ornithine 4,5-Aminomutase and Methylmalonyl-CoA Mutase

Caitlyn Makins, Alex V. Pickering, Chloe Mariani, and Kirsten R. Wolthers*

Department of Chemistry, University of British Columbia, 3333 University Way, Kelowna, BC V1V 1V7, Canada

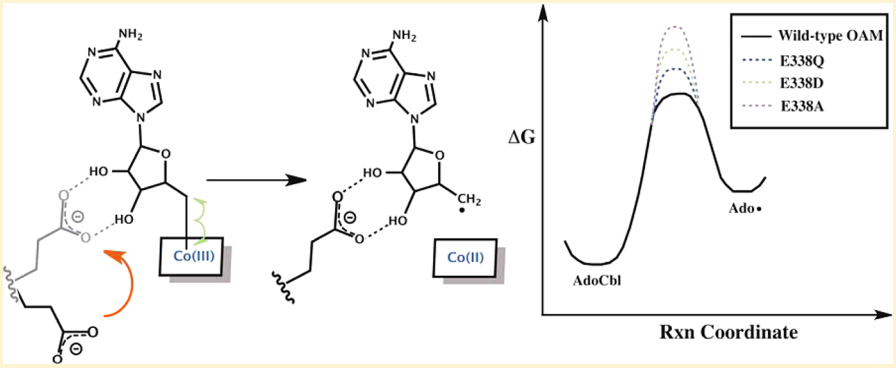

ABSTRACT: Binding of substrate to ornithine 4,5-aminomutase (OAM) and methylmalonyl-CoA mutase (MCM) leads to the formation of an electrostatic interaction between a conserved glutamate side chain and the adenosyl ribose of the adenosylcobalamin (AdoCbl) cofactor. The contribution of this residue (Glu338 in OAM from *Clostridium sticklandii* and Glu392 in human MCM) to AdoCbl Co−C bond labilization and catalysis was evaluated by substituting the residue with a glutamine, aspartate, or alanine. The OAM variants, E338Q, E338D, and E338A, showed 90-, 380-, and 670-fold reductions in catalytic turnover and 20-, 60-, and 220-fold reductions in k_{cat}/K_m, respectively. Likewise, the MCM variants, E392Q, E392D, and E392A, showed 16-, 330-, and 12-fold reductions in k_{cat}, respectively. Binding of substrate to OAM is unaffected by the single-amino acid mutation as stopped-flow absorbance spectroscopy showed that the rates of external aldimine formation in the OAM variants were similar to that of the native enzyme. The decrease in the level of catalysis is instead linked to impaired Co−C bond rupture, as UV−visible spectroscopy did not show detectable AdoCbl homolysis upon binding of the physiological substrate, D-ornithine. AdoCbl homolysis was also not detected in the MCM mutants, as it was for the native enzyme. We conclude from these results that a gradual weakening of the electrostatic energy between the protein and the ribose leads to a progressive increase in the activation energy barrier for Co−C bond homolysis, thereby pointing to a key role for the conserved polar glutamate residue in controlling the initial generation of radical species.

Adenosylcobalamin (coenzyme B_{12}, AdoCbl)-dependent enzymes catalyze radical-mediated isomerizations in which a hydrogen atom is exchanged with a variable group on a vicinal carbon atom (Figure 1).[1,2] AdoCbl is the source of radicals as binding of substrate to the enzyme induces homolytic cleavage of the cofactor's unusual cobalt−carbon (Co−C) bond, generating cob(II)alamin and a 5′-deoxyadenosyl radical (Ado•). The latter highly reactive species abstracts a hydrogen atom from the substrate producing 5′-deoxyadenosine (AdoH) and a carbon-centered substrate radical, which isomerizes to a productlike radical intermediate. The latter half of the catalytic cycle entails re-abstraction of hydrogen from the C5′ atom of 5′-deoxyadenosine by the product radical intermediate and re-formation of AdoCbl through recombination of cob(II)alamin and the 5′-deoxyadenosyl radical.

The core structural motifs of AdoCbl-dependent enzymes, with the exception of class II ribonucleotide reductase,[3] are a Rossmann-like domain that coordinates to the distal side of the AdoCbl cofactor and an $(\alpha/\beta)_8$ TIM barrel that houses the substrate binding site. The family falls into three subclasses according to the mode of AdoCbl binding, cofactor requirement, and the nature of the migrating group. Carbon skeleton rearrangements are performed by the class I mutases (e.g., methylmalonyl-CoA mutase[4] and glutamate mutase).[5] The class II eliminases (diol dehydratase,[6] glycerol dehydratase, and ethanolamine ammonia lyase[7]) catalyze the migration and subsequent elimination of a heteroatom. Finally, class III aminomutases (ornithine 4,5-aminomutase[8] and lysine 5,6-aminomutase[9]) require pyridoxal 5′-phosphate (PLP) to perform a 1,2-amino shift.

Structural and spectroscopic studies of members of all three subclasses reveal that substrate binding induces structural

Received: September 17, 2012
Revised: December 18, 2012
Published: January 11, 2013

   dx.doi.org/10.1021/bi3012719 | *Biochemistry* 2013, 52, 878−888

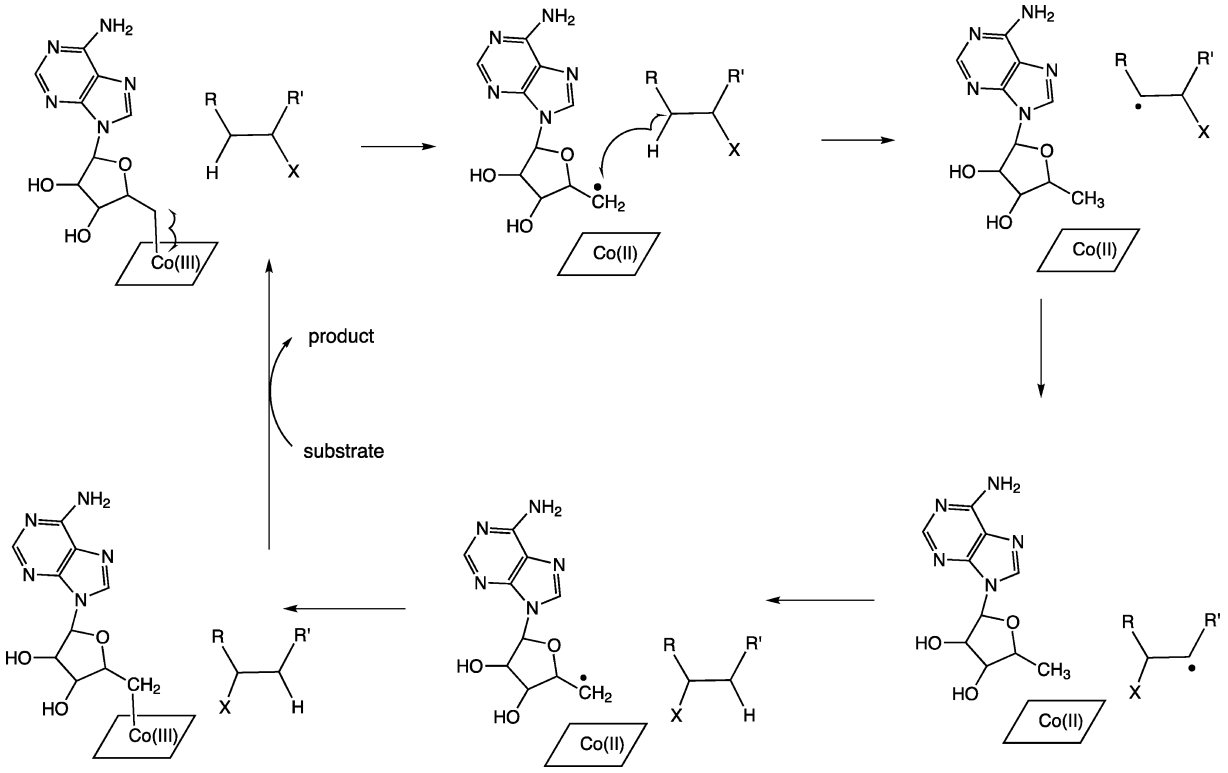

Figure 1. Generalized catalytic cycle for 1,2-rearrangements catalyzed by AdoCbl-dependent enzymes. Substrate binding induces Co−C bond homolysis forming cob(II)alamin and a 5′-deoxyadenosyl radical (Ado•). With the exception of AdoCbl-dependent ribonucleotide reductase, in which hydrogen abstraction by the 5′-deoxadenosyl radical generates an active site thiyl radical, the Ado• abstracts a hydrogen from the substrate to form a substrate−radical intermediate and 5′-deoxyadenosine (AdoH). Isomerization leads to a product−radical intermediate, which then re-abstracts hydrogen from AdoH. Release of product and re-formation of the Co−C bond complete the cycle.

rearrangements in the protein scaffold.[10−14] The most extreme example of this occurs with the aminomutases. Recent computational calculations of ornithine 4,5-aminomutase (OAM) show that the Rossmann domain undergoes an ∼52° rotation and an ∼14 Å translation upon binding of the substrate.[15] In the substrate-free form of OAM, the Rossmann domain is tilted toward the edge of the TIM barrel, exposing the 5′-deoxyadenosyl moiety of AdoCbl to the solvent (Figure 2A).[16] The PLP cofactor, noncovalently bound to the TIM barrel active site, forms an internal aldimine with a lysine originating from the Rossmann domain. This protein−cofactor covalent link effectively locks the enzyme into an "edge-on" conformation, separating the PLP and 5′-deoxyadenosyl moiety by ∼23 Å. The incoming substrate displaces the internal aldimine, forming an external aldimine link via its migrating amine group. This first step of the catalytic cycle is anticipated to free the Rossmann domain to rotate toward the TIM barrel to form the "top-on" conformation, as observed in the crystal structures of the mutases (Figure 2B).[17,18] Positioning of AdoCbl into the active site triggers Co−C bond homolysis, and the ensuing radical chemistry allows OAM (from *Clostridium sticklandii*) to convert D-ornithine to (2*R*,4*S*)-2,4-diaminopentanoic acid.

Although the aminomutases have not been structurally captured in the top-on arrangement, evidence that they populate this conformational state during catalysis is provided by electron paramagnetic resonance (EPR) spectra of OAM[12] and 5,6-LAM[13] in the presence of substrate analogues. Modeling of OAM into the top-on state, via rigid-body alignment of the TIM barrels of OAM (PDB entry 3KOZ) and glutamate mutase (PDB entry 1I9C), generates a plausible catalytically ready conformation, as it places C5′ of Ado in optimal alignment for abstraction of a hydrogen atom from the C4 atom of the ornithinyl-PLP complex.[15,16] The top-on model also reveals a Glu γ-carboxylate (Glu338) in position for polar contact with the 2′-OH and 3′-OH of the 5′-deoxyadenosyl ribose moiety (Figure 2C). Glu338 of OAM in the top-on model superimposes with Glu330 of glutamate mutase (GM),[19] highlighting the residue's potential catalytic role in both the class I and class III isomerases.

Methylmalonyl-CoA mutase (MCM) interconverts methylmalonyl-CoA to succinyl-CoA, an activity that, in mammals, is key for the catabolism of cholesterol, odd-chain fatty acids, and branched-chain amino acids.[20] In the substrate-free structure of MCM (Figure 2B), the Rossmann-like domain is positioned directly above the pore of the TIM barrel, such that the 5′-deoxyadenosyl moiety is occluded from the bulk solvent and near the active site.[17] Despite the low level of sequence homology, this overall domain organization and top-on configuration is seemingly conserved within carbon-skeleton mutases.[18] Methylmalonyl-CoA enters the MCM active site via the opposite end of the TIM barrel, inducing structural rearrangements that globally amount to a constriction and tightening of the TIM barrel channel.[11,21] Several conserved residues lining the channel form new contacts with the substrate and/or cofactor. Of particular note is Glu392, which rotates upon substrate binding to form new polar interactions with the ribose 2′-OH and 3′-OH (Figure 2D), adopting a conformation similar to that of Glu330 in GM and Glu338 in the top-on model conformation of OAM. Formation of this

dx.doi.org/10.1021/bi3012719 | *Biochemistry* 2013, 52, 878−888

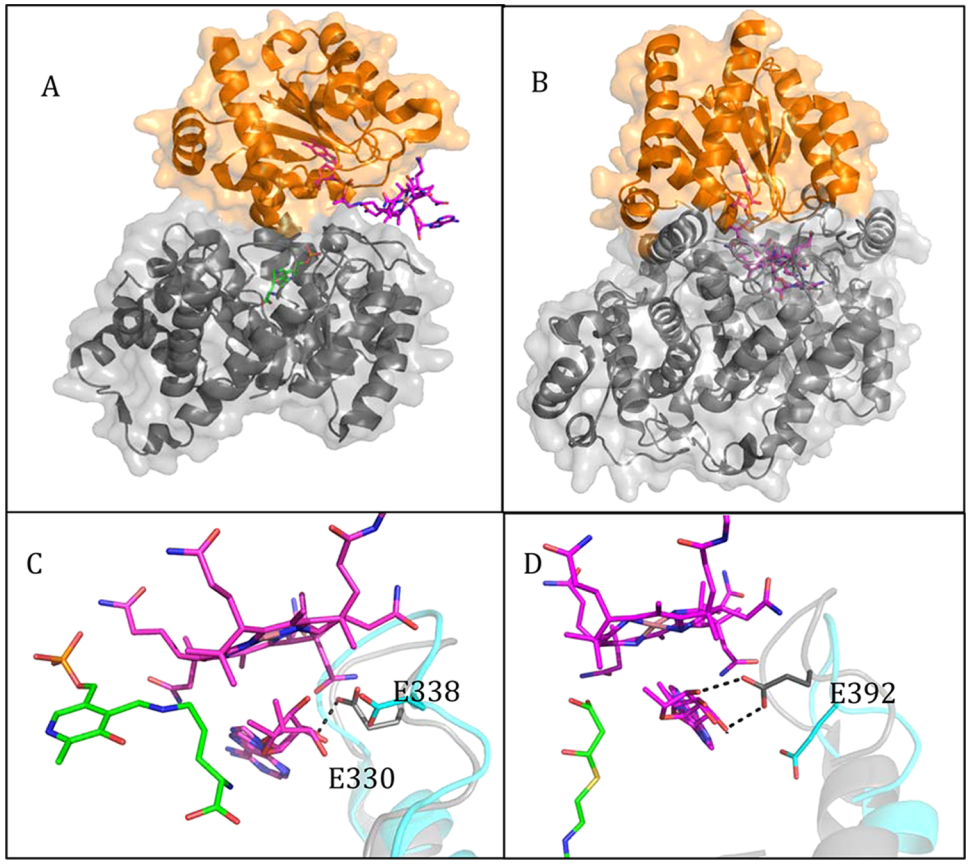

Figure 2. Conformational changes observed in OAM and MCM upon substrate binding. (A) The edge-on conformation of the Rossmann domain (orange) with respect to the TIM barrel (gray) in OAM (PDB entry 3KOZ) exposes the proximal face of AdoCbl and separates the 5′-deoxyadenosyl moiety of AdoCbl (magenta) form the PLP cofactor (green) by 23 Å. (B) Structure of substrate-free MCM illustrating the top-on conformation that buries AdoCbl in the protein core (PDB entry 2XIJ). The coloring scheme is the same as that for panel A. (C) Active site of the modeled closed or top-on conformation of OAM (gray) with the ornithinyl-PLP complex (green), showing the relative orientation of Glu338 with respect to the 5′-deoxyadenosyl ribose moiety. Colored cyan is the superimposed TIM barrel of glutamate mutase (PDB entry 1I9C) showing a similarly positioned glutamate residue (Glu330). (D) Superposition of substrate-free MCM (cyan; PDB entry 2XIJ) and the MCM–methylmalonyl-CoA complex (gray; PDB entry 2XIQ) showing rotation of E392 and the formation of polar contacts with the 5′-deoxyadenosyl moiety. Methylmalonyl-CoA is represented as green sticks.

new noncovalent contact between the protein and cofactor is hypothesized, from computational calculations, to lower the activation energy barrier to Co–C bond homolysis in MCM by contributing to electrostatic stabilization of the 5′-deoxyadenosyl radical.[22,23] This residue, located in a loop between α8 and β8 of the TIM barrel, is conserved across AdoCbl-dependent mutases, with sequences 4–39% similar to that of MCM (Figure 3). Given that the ribose-coordinated glutamate potentially plays a catalytic role, we have mutated this residue to an alanine, glutamine, or aspartate in OAM and human MCM. Our results show that the residue does contribute to Co–C bond homolysis in OAM and MCM, suggesting a conserved mechanism for radical initiation in mutases and aminomutases.

MCM	TQSLHTNSFDEALGLPTV	399
HCM	AQSLHTNGYDEAFAIPTE	379
ICM	TNSLHTNALDETLALPSE	369
ECM	ARAVQLPAWNEALGLPRP	307
GM	ATKVIVKTPHEAIGIPTK	337
MAM	ADKIITKTKQEASGIPTK	323

Figure 3. Multiple-sequence alignment of different AdoCbl mutases showing the conserved glutamate residue: human methylmalonyl-CoA mutase (AAA59569.1), HCM (hydroxisobutyryl-CoA mutase) from *Methylibium petroleiphilum* (YP_001023546.1), ICM (isobutyryl-CoA mutase) from *Streptomyces clavuligerus* (EFG09395.1), ECM (ethylmalonyl-CoA mutase) from *Rhodobacter sphaeroides* (YP_354045.1), GM (glutamate mutase) from *Clostridium tetanomorphum* (CAA49910.1), and MAM (methylaspartate mutase) from *Arcobacter nitrofigilis* (ADG93549.1). Relative to human MCM, the levels of sequence similarity are as follows: 39% for HCM, 38% for ICM, 33% for ECM, 4% for GM, and 4% for MAM.

EXPERIMENTAL PROCEDURES

Materials. AdoCbl, PLP, D-ornithine, DL-2,4-diaminobutyric acid, GDP, DTNB, and methylmalonyl-CoA were obtained from Sigma. The Ni^{2+}-nitrilotriacetic acid (Ni-NTA) column and Q-Sepharose High Performance resins were from GE Biosciences. Restriction endonucleases were from New England Biolabs; *Pfu* Turbo DNA polymerase was from Agilent Technologies, and Rosetta(DE3)pLysS competent cells were purchased from EMD Biosciences. Thiokinase (succinyl-CoA synthetase) was purchased from Cedarlane Laboratories. All other chemicals were purchased from Fisher Scientific and were of the highest grade available.

dx.doi.org/10.1021/bi3012719 | *Biochemistry* 2013, 52, 878–888

Construction of MCM and OAM Mutants. The OAM and MCM single-point mutations described in this paper were introduced into the pOAMH2[12] and pNIC-CTHF vectors,[21] respectively, using the QuikChange site-directed mutagenesis method (Agilent Technologies, Mississauga, ON). The DNA Sequencing Laboratory at University of British Columbia (Vancouver, BC) sequenced each mutant to verify that the mutation was successfully engineered into the construct and to confirm that no other polymerase chain reaction-induced errors had occurred.

Enzyme Purification. The OAM mutants and wild-type DAPDH were purified as previously described.[12,24] The plasmid construct containing the coding sequence for human MCM, pNIC-CTHF, was obtained from the Structural Genomics Consortium (Oxford, U.K.). A hexahistidine tag was engineered onto the C-terminus of the MCM cDNA in the pNIC-CTHF construct allowing for purification of the recombinant protein by Ni^{2+}-NTA affinity chromatography. Wild-type MCM and the engineered point mutants were transformed into *Escherichia coli* Rosetta(DE3)pLysS cells, and the proteins were expressed as described previously.[21]

MCM was purified as described with minor modifications.[21] Rosetta(DE3)pLysS cells (24 g, wet weight) overexpressing MCM were resuspended in 200 mL of 50 mM HEPES-KOH (pH 7.5), 5% glycerol, 10 mM imidazole, 0.5 mM TCEP, and 0.1 mM PMSF. Cells were disrupted by sonication (5 s pulses separated by a 50 s interval for 30 min, power setting of 22%) using a Misonix sonicator. The cell suspension was clarified by centrifugation at 39000*g* for 45 min. The supernatant, following the addition of sodium chloride (0.5 M), was applied to a 5 mL Ni^{2+}-nitrilotriacetic acid (Ni^{2+}-NTA) column equilibrated with 50 mM HEPES-KOH (pH 7.5), 0.5 M NaCl, 0.5 mM TCEP, and 10 mM imidazole. The column was washed with 30 mL of 50 mM HEPES-KOH, 0.5 M NaCl (pH 7.5), and 10 mM imidazole, and then 25 mL of 50 mM HEPES-KOH, 0.5 M NaCl (pH 7.5), and 40 mM imidazole. The protein was eluted via application of 25 mL of 50 mM HEPES-KOH, 0.5 M NaCl (pH 7.5), and 350 mM imidazole to the Ni^{2+}-NTA column. Fractions containing MCM were pooled and diluted 5-fold with 50 mM HEPES-KOH (pH 7.5) and directly applied to a 60 mL Q-Sepharose HP column (2.6 cm × 11 cm) equilibrated with 50 mM HEPES-KOH (pH 7.5). The column was washed with 120 mL of 50 mM HEPES-KOH (pH 7.5), and the protein was eluted with a 1.2 L linear gradient to 0.5 M NaCl at a flow rate of 2 mL/min. Fractions containing purified MCM, as judged by an absorbance reading at 280 nm and sodium dodecyl sulfate−polyacrylamide gel electrophoresis analysis, were pooled and concentrated using Centricons with a 30 kDa molecular mass cutoff filter. Concentrated protein samples containing 20% glycerol were then flash-frozen in liquid nitrogen and stored at −80 °C. Protein concentrations were determined by the Lowry method using bovine serum albumin as a standard.

Coupled Enzyme Assays. OAM activity was measured using a coupled spectrophotometric assay with DAPDH as previously described.[24] Data from the substrate concentration dependence experiments were fit to the Michaelis−Menten equation. MCM activity was measured using a coupled spectrophotometric assay with thiokinase (succinyl-CoA synthetase), as previously described,[25] with the exception that 50 mM Tris buffer (pH 7.5) was used in place of a Tris phosphate buffer (pH 7.5) (50 mM in phosphate). The total volume of the reaction mixture was 300 μL. Saturating concentrations of (*R*,*S*)-methylmalonyl-CoA were used to obtain average k_{cat} values for wild-type MCM as well as the E392Q, E392D, and E392A mutants. The background activity at 412 nm prior to addition of MCM was recorded for 5 min and subtracted from the activity recorded over 5 min following the addition of MCM. Assays were performed in triplicate at 30 °C to obtain the reported turnover rate.

Aerobic and Anaerobic UV−Visible Spectroscopy. UV−visible spectral assays were performed on a Perkin-Elmer Lambda 25 spectrophotometer at 25 °C. The 1 mL reaction mixtures contained 15 μM apo-OAM, 15 μM PLP, and 15 μM AdoCbl in 100 mM NH_4^+EPPS (pH 8.5). The reaction was initiated via the addition of 2.5 mM D-ornithine or 2.5 mM DL-2,4-diaminobutryic acid, and the spectra were recorded from 700 to 300 nm every minute for 90 min. For spectra recorded under anaerobic conditions, 2 mL of concentrated apo-OAM (50 μM) was introduced into an anaerobically maintained glovebox (Belle Technology) and gel filtered over a 10 mL PD10 column equilibrated with anaerobic buffer [100 mM NH_4^+EPPS (pH 8.5)]. Solutions of AdoCbl and PLP (prepared in the glovebox with anaerobic buffer) were added in stoichiometric amounts to the apoprotein. The UV−visible absorbance spectra of the holo-OAM solution were recorded in a septum-sealed cuvette with the Perkin-Elmer Lambda 25 spectrophotometer at 25 °C. An anaerobic solution of 2.5 mM D-ornithine or 2.5 mM DL-2,4-diaminobutyric acid was then titrated into the cuvette, and the optical spectra were recorded every min for 90 min.

Stopped-Flow Spectroscopy. Anaerobic stopped-flow studies were performed using an SF-61DX2 stopped-flow instrument (TgK Scientific). The sample-handling unit of the stopped-flow instrument was housed in a specialized glovebox (Belle Technology) in which the O_2 concentration was <5 ppm. Anaerobic solutions of buffer, enzyme, cofactors, substrate, and substrate analogues were prepared as previously described.[12] For the OAM mutants, transient kinetic experiments were performed in 100 mM NH_4^+EPPS (pH 8.5) at 25 °C. The cofactors PLP and AdoCbl were added to the apoenzyme in equimolar concentrations to form the holoenzyme. Holo-OAM (50 μM) was rapidly mixed with 5 mM D-ornithine or DL-2,4-diaminobutyrate, and transimination and Co−C bond homolysis were followed at 416 and 528 nm, respectively.

MCM pre-steady-state analysis was performed in 50 mM potassium phosphate buffer (pH 7.5) at 10 °C. Holo-MCM was generated by adding an equimolar amount of AdoCbl to the apoenzyme, and then a 50 μM solution of holoenzyme was rapidly mixed with 1 mM methylmalonyl-CoA. AdoCbl homolysis was monitored following a change in absorbance at 525 nm. Concentrations of the holoenzyme, substrate, and substrate analogue in the text and figure legends refer to syringe concentrations (i.e., before the mixing event). The substrate, substrate analogue, and holoenzymes were diluted 2-fold after the mixing event. Eight to ten absorbance traces were averaged and then fit to a single-exponential equation to extract observed rate constants.

Adenosylcobalamin Equilibrium Binding Assay. Fluorescence spectroscopy was used to determine the equilibrium dissociation constant of AdoCbl following a previously published protocol.[9] The assays were performed on a Perkin-Elmer LS45 fluorescence spectrometer with excitation and emission slit widths of 10.0 nm. The assay relies on quenching of the intrinsic tryptophan residues that occurs with binding of AdoCbl to the protein. Sequential additions of 2−4 μL of a

dx.doi.org/10.1021/bi3012719 | *Biochemistry* 2013, 52, 878−888

concentrated AdoCbl stock were made to a 3 mL quartz fluorescence cuvette with 2980 μL of either 0.04 or 0.056 μM apo-MCM, yielding AdoCbl concentrations that ranged from 0.04 to 0.96 μM. The titration was performed in 50 mM potassium phosphate buffer (pH 7.5). After each AdoCbl addition, the cuvette was inverted several times and incubated for 20 min at 3.2 °C. Tryptophan residues were then excited at 282 nm, and fluorescence emission was detected between 300 and 380 nm. Five scans (240 nm/min) at each AdoCbl concentration were averaged. The change in the fluorescence emission at 340 nm was fit to the quadratic binding isotherm (eq 1).

$$\Delta F = \left(\frac{\Delta F_{max}}{2E_o}\right)\{E_o + L_o + K_d - [(E_o + L_o + K_d)^2 - 4E_oL_o]^{1/2}\} \quad (1)$$

where L_o is the total AdoCbl concentration, E_o is the total enzyme concentration, ΔF is the change in fluorescence, ΔF_{max} is the maximal change in fluorescence emission, and K_d is the dissociation constant for the AdoCbl−MCM complex.

RESULTS

Steady-State Kinetic Properties of the OAM Mutants. Catalytic turnover for wild-type OAM was previously monitored through a coupled spectrophotometric assay in which reduction of NAD^+ to NADH was followed by an absorbance increase at 340 nm. [24] The coupling enzyme is 2,4-diaminopentanoic acid dehydrogenase (DAPDH), which catalyzes the NAD^+-dependent oxidative deamination of 2,4-diaminopentanoic acid (product of OAM turnover) to 2-amino-4-ketopentanoate. Wild-type OAM displayed a turnover number of 2.9 ± 0.1 s^{-1} and a K_m value of 190 ± 13 μM for D-ornithine.[24] Substitution of Glu338 with a Gln, whereby the potential for electrostatic interactions with the 2′- and 3′-hydroxyl groups of the ribose moiety is retained, resulted in a 90-fold reduction in k_{cat} (Table 1). Displacement of the terminal carboxyl functional group by a distance of ∼2 Å, through mutation of Glu338 to Asp, resulted in a more substantial 380-fold decrease in the rate of catalytic turnover. The most profound effect on k_{cat}, a 670-fold decrease, was observed when the polar side chain was removed altogether in the E338A mutant. The K_m value for D-ornithine is 42.7 ± 3.3, 30.2 ± 2.1, and 60.6 ± 4.9 μM for the E338Q, E338D, and E338A mutants, respectively. As a result of the altered k_{cat} and K_m values, the catalytic efficiency (k_{cat}/K_m) of each of the mutants was decreased in comparison to that of wild-type OAM. Following the same trend observed for catalytic turnover, the E338Q, E338D, and E338A mutants showed 20-, 60-, and 220-fold reductions in k_{cat}/K_m, respectively.

Table 1. Summary of Steady-State Kinetic Parameters for Wild-Type OAM and the E338 Variants

enzyme	k_{cat} (s^{-1})	K_m(D-Orn) (μM)	k_{cat}/K_m(D-Orn) ($\times 10^3$ M^{-1} s^{-1})
wild type	2.9 ± 0.1	190 ± 13	15.2 ± 1.2
E338A	4.3 ± 0.1 × 10^{-3}	60.6 ± 4.9	0.07 ± 0.01
E338Q	0.032 ± 0.001	42.7 ± 3.3	0.75 ± 0.08
E338D	7.6 ± 0.1 × 10^{-3}	30.2 ± 2.1	0.25 ± 0.02

Steady-State Kinetic Properties of the MCM Mutants. MCM catalytic activity was measured by a continuous spectrophotometric assay using the coupling enzyme thiokinase (succinyl-CoA synthetase).[25] Thiokinase converts succinyl-CoA to succinate and CoA in a GDP-dependent fashion. Wild-type MCM displayed a turnover number of 3.9 ± 0.1 s^{-1} at 30 °C, similar to that reported for MCM from *Propionibacterium shermanii*.[26] The E392Q, E392D, and E392A mutants showed 16-, 330-, and 12-fold reductions in the rate of catalytic turnover compared to that of the native enzyme, respectively (Table 2).

Table 2. Summary of Catalytic Turnover Rates Observed for Wild-Type MCM and the E392Q, E392D, and E392A Mutants

enzyme	k_{cat} (s^{-1})
wild type	3.95 ± 0.11
E392Q	0.25 ± 0.01
E392D	0.012 ± 0.001
E392A	0.32 ± 0.02

Absorption Spectra of the OAM Mutants. Holo-OAM (wild-type OAM with PLP and AdoCbl) has a characteristic UV−visible spectrum with prominent contributions from both the PLP (at 416 nm) and AdoCbl (at 528 nm) cofactors.[12] The binding of the physiological substrate D-ornithine results in an initial transimination event to form the external aldimine. This is observed spectrally as a decrease in absorbance at 416 nm and the formation of an absorbance peak at 425 nm. Substrate binding also induces Co−C bond homolysis as demonstrated by a small absorbance decrease at 528 nm. While Co−C bond homolysis is evident, both UV−visible and electron paramagnetic resonance (EPR) spectroscopic techniques have been unable to detect a steady-state accumulation of the cob(II)alamin species (absorbance peak at 470 nm) because of the instability of ornithinyl-PLP-derived radical species. In contrast, binding of the inhibitor DL-2,4-diaminobutyric acid (DABA) to OAM results in a significant decrease in absorbance at 528 nm and the formation of a discrete peak at 470 nm.[12] The chemical nature of the persistent 2,4-diaminobutyryl-PLP-derived radical is discussed later.

To determine the effects of the mutations on transimination and Co−C bond homolysis, UV−visible spectra were obtained for the OAM variants (in holoenzyme form) when they were mixed with D-ornithine and DABA under anaerobic and aerobic conditions. The anaerobic conditions allow for detection of a stable biradical state with the inhibitor, while the aerobic conditions allow monitoring of cob(III)alamin formation. The interception of the cob(II)alamin intermediate by O_2 leads to the formation of cob(III)alamin, and this reaction, leading to enzyme inactivation, is noted by an increase in absorbance at 358 nm. For native OAM, cob(III)alamin formation occurs at a rate of 0.4 min^{-1} in the presence of substrate.[24]

Figure 4A shows the spectral shift in the holoenzyme form of E338Q upon addition of D-ornithine under aerobic conditions. The decrease in absorbance at 416 nm reflects transimination, but the lack of an absorbance decrease at 528 nm points to impaired Co−C bond homolysis. The absence of cob(III)alamin formation, even after 90 min, further suggests that generation of the cob(II)alamin intermediate by activation of AdoCbl is affected by the mutation. Similar spectral transitions were observed upon binding of D-ornithine to all three OAM variants under aerobic and anaerobic conditions.

dx.doi.org/10.1021/bi3012719 | *Biochemistry* 2013, 52, 878−888

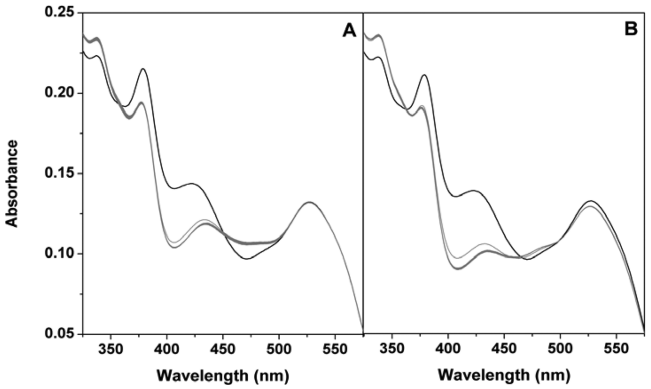

Figure 4. Changes in the UV−visible absorbance spectra of the OAM E338Q mutant upon binding of D-ornithine and DL-2,4-diaminobutyrate. The holoenzyme reaction mixture contained 15 μM OAM, 15 μM PLP, and 15 μM AdoCbl in 100 mM NH_4^+EPPS pH 8.5. (A) Spectral changes for E338Q recorded before (black line) and after (gray lines) the addition of 5 mM D-ornithine under aerobic conditions. Similar spectral transitions were observed under aerobic conditions and with E338D and E338A. (B) Spectral changes for E338Q recorded before (black line) and after (gray lines) the addition of 5 mM 2,4-diaminobutyrate under anaerobic conditions. Similar spectral transitions were observed under aerobic conditions and with E338D and E338A. For both panels A and B, optical changes were monitored every 2 min for 1 h. Only representative spectra are shown.

Figure 4B shows a shift in the holoenzyme absorbance spectra for OAM E338Q with the addition of DABA under anaerobic conditions. Similar spectral transitions were observed for all three mutants, with or without O_2 in the reaction mixture. As with D-ornithine, the binding of DABA results in external aldimine formation (decrease at 416 nm), but unlike studies with the physiological substrate, there was a small decrease in absorbance at 528 nm suggesting limited Co−C bond homolysis. However, the usual buildup of the cob(II)-alamin species (at 470 nm) observed in the wild-type OAM−DABA complex was absent in all three mutants. Moreover, there was no accumulation of cob(III)alamin over 90 min, even in the presence of O_2. Overall, these studies suggest that substitution of Glu338 does not affect the formation of the external aldimine but does impair subsequent radical initiation by the AdoCbl cofactor.

Stopped-Flow Analysis of OAM Variants. Stopped-flow experiments have previously been used to measure rates of Co−C bond homolysis (absorbance decrease at 528 nm) and transimination (absorbance decrease at 416 nm) in holo-OAM upon addition of both D-ornithine and the substrate analogue, DL-2,4-diaminobutyric acid.[12] Observed rate constants for Co−C bond homolysis and transimination were found to be on the same order of magnitude (~500 s^{-1}) with both the substrate and inhibitor. Figure 5 shows that all three Glu338 mutants elicited rates of transimination with DABA similar to that of wild-type OAM. A monoexponential fit of the absorbance traces at 416 nm (1−20 ms) produced rate constants of 514 ± 26, 577 ± 66, and 454 ± 36 s^{-1} for E338Q, E338D, and E338A mutants, respectively. In the absence of bound AdoCbl (i.e., with only PLP bound to the protein), the transimination rates are much slower (2500-fold) for the native enzyme.[12] Thus, the fact that these calculated rate constants are unchanged in the OAM mutants suggests that AdoCbl binding is unaffected by the single-point mutation, as impaired AdoCbl binding would likely result in slower rates of transimination.

The Co−C bond homolysis signal at 528 nm was detected upon rapid mixing of the native enzyme with DABA, giving an observed rate constant of 489 ± 40 s^{-1} (Figure 6). Consistent with the UV−visible spectral binding data, rapid mixing of the OAM variants with D-ornithine did not result in an absorbance decrease at 528 nm. Rapid mixing with DABA also did not reproducibly show a homolysis signal at 528 nm (data not shown). Given the small absorbance change in the AdoCbl cofactor that is generated by binding of the inhibitor to the

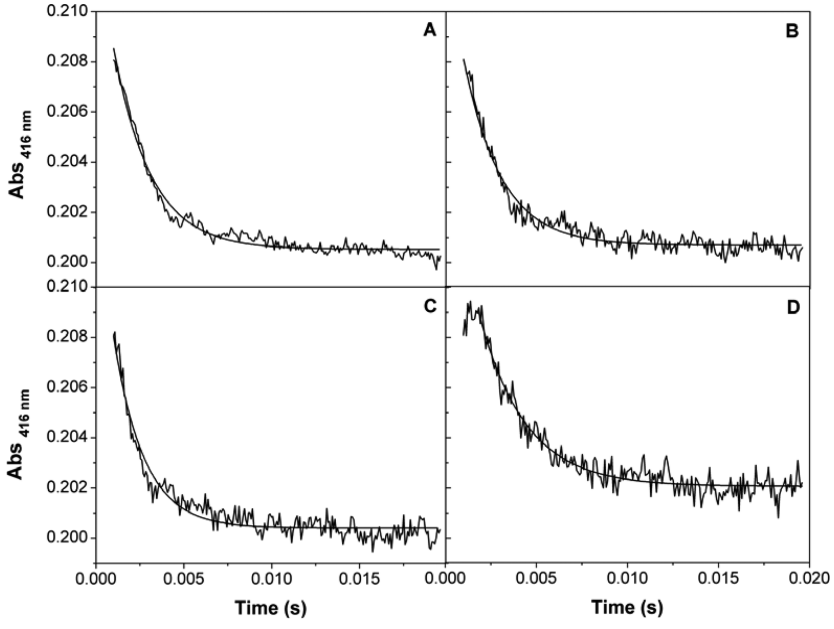

Figure 5. Stopped-flow absorbance changes following transimination in OAM. The transimination event was monitored at 416 nm over 20 ms following rapid mixing of 50 μM wild-type (A), E338Q (B), E338D (C), and E338A (D) with 5 mM DABA, under anaerobic conditions as described in Experimental Procedures. An average of 8−10 traces were fit to a single-exponential equation to generate the observed rate constants for transimination of 464 ± 36, 514 ± 26, 577 ± 66, and 454 ± 36 s^{-1} for the wild type, E338Q, E338D, and E338A, respectively.

dx.doi.org/10.1021/bi3012719 | *Biochemistry* 2013, 52, 878−888

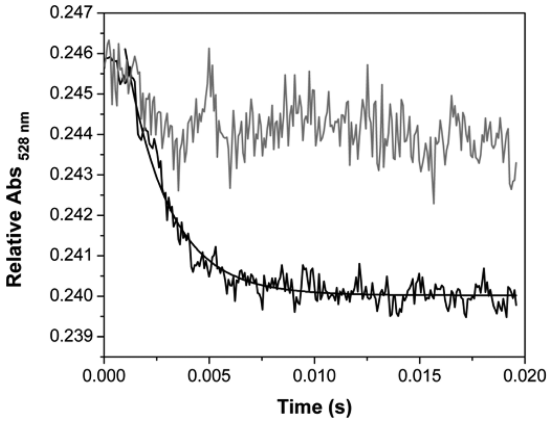

Figure 6. Stopped-flow absorbance changes following Co−C bond homolysis in OAM. The Co−C bond homolysis event was monitored at 528 nm over 20 ms following rapid mixing of 50 μM wild type (black line) with 5 mM DABA. As in Figure 4, an average of 8−10 traces were fit to a single-exponential equation to generate the observed rate constant of 489 ± 40 s^{-1} for homolysis. No detectable homolysis signal was detected for E338Q (gray trace) or the other two mutants (data not shown).

holoenzyme mutants under steady-state conditions, it is unlikely that we would be able to reliably detect this homolysis signal in the stopped-flow given the low signal-to-noise ratio of the instrument. These combined stopped-flow data indicate that the mutations do not compromise the rate of external aldimine formation or AdoCbl binding, but they do significantly impair radical generation, possibly by shifting the internal equilibrium of the Co−C bond homolysis step toward the intact cofactor.

Stopped-Flow Analysis of MCM. Analogous stopped-flow experiments were conducted with MCM (wild type and mutants) to determine if the corresponding residue (E392) activates radical chemistry. The observed rate constant for homolysis in wild-type MCM upon mixing with methylmalonyl-CoA at 10 °C was found to be 657 ± 29 s^{-1} (Figure 7A), similar to previously published results.[27] Recombination of the cofactor (absorbance increase at 525 nm) following depletion of the substrate in the reaction cell was observed after 8 s (Figure 7B). As with the OAM Glu338 mutants, no homolysis signal was detected in any of the E392 mutants upon mixing with methylmalonyl-CoA (only absorbance traces for E392D are shown). These results point to a universal role of the highly conserved Glu in triggering AdoCbl homolysis in class I and class III isomerases.

Adenosylcobalamin Binding Assays for MCM. The effect of mutating Glu392 in MCM on AdoCbl binding was assessed through a fluorescence binding assay. Previously, it was shown that binding of AdoCbl to MCM results in a quenching of the intrinsic tryptophan fluorescence. Figure 8 shows a decrease in the fluorescence emission at 340 nm as AdoCbl is gradually added to both the native enzyme and E392D. To extract equilibrium dissociation constants for both proteins, the

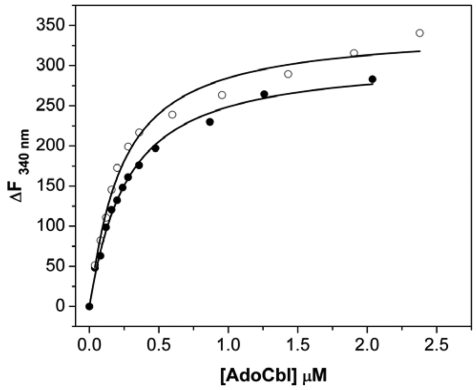

Figure 8. Determination of the equilibrium dissociation constant for AdoCbl for wild-type MCM and E392D. Native MCM [0.056 μM (●)] and E392D [0.040 μM (○)] were titrated with AdoCbl (0.04−0.96 μM) at 3.2 °C in 50 mM potassium phosphate buffer (pH 7.5) as described in Experimental Procedures. The change in fluorescence at 340 nm is plotted vs the total concentration of AdoCbl, and the data were fit to eq 1 (—), keeping the total enzyme concentration fixed at 0.056 μM for MCM and 0.040 μM for E392D. The K_d was determined to be 0.21 ± 0.02 μM for native MCM and 0.23 ± 0.02 μM for E392D.

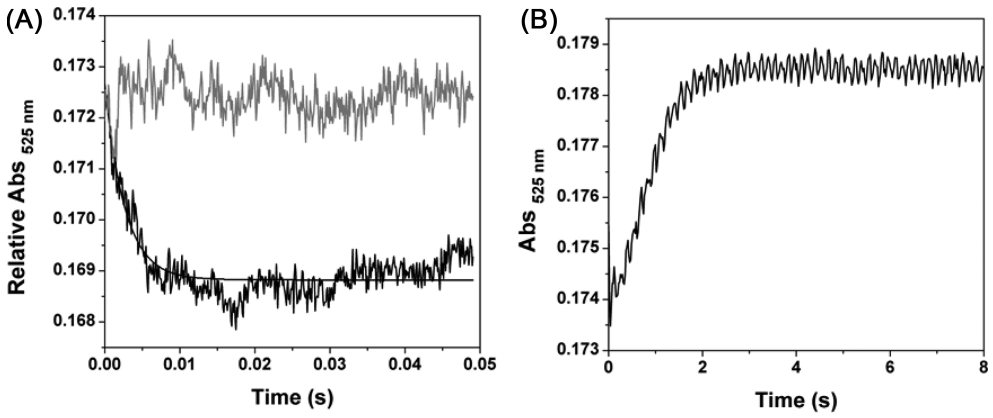

Figure 7. Stopped-flow absorbance changes following Co−C bond homolysis in holo-MCM upon mixing with methylmalonyl-CoA. (A) The Co−C bond homolysis step was monitored at 525 nm over 50 ms at 10 °C under anaerobic conditions as described in Experimental Procedures. An average of 5−10 traces was fit to a single-exponential equation, giving an observed rate constant of 657 ± 29 s^{-1} for wild-type methylmalonyl-CoA mutase. No homolysis signal was detected for E392D (gray line) or the other two mutants (not shown). (B) Absorbance changes observed at 525 nm over 8 s following rapid mixing of 50 μM wild-type MCM with 1 mM methylmalonyl-CoA. The increase in absorbance at 525 nm reflects re-formation of the Co−C bond following consumption of the substrate. Analogous absorbance increases at 525 nm were not observed in any of the three MCM mutants.

dx.doi.org/10.1021/bi3012719 | *Biochemistry* 2013, 52, 878−888

data were fit to the quadratic binding isotherm (eq 1), keeping the total concentration of each enzyme fixed. Native MCM generated an apparent K_d of 0.23 ± 0.01 μM for AdoCbl, which is similar to that of E392D (0.21 ± 0.02 μM) and previously published data.[28] The absence of a significant shift in the equilibrium dissociation constant suggests that mutation of the Glu392 side chain does not perturb cofactor binding.

DISCUSSION

The origin of the enormous rate enhancements achieved by enzymes continues to be an actively investigated and debated area of science, fed increasingly by the desire to design protein scaffolds capable of chemical reactions that are of industrial or therapeutic use. Adenosylcobalamin-requiring enzymes are one of the model systems that have been used by experimental and computational chemists to examine the basis for enzymatic catalytic prowess.[4,22,29−31] In solution, the rate of AdoCbl bond homolysis is 10^{-9} s^{-1} at 25 °C; however, stopped-flow spectroscopy reveals that the rate constant for Co−C bond homolysis in MCM and OAM is >600 s^{-1}.[7,12,27,32] For MCM and glutamate mutase, primary kinetic isotope studies with deuterated substrates indicate that Ado• formation is kinetically coupled to hydrogen abstraction,[27,32] but there is debate about whether Co−C bond homolysis and abstraction of hydrogen from the substrate follow a stepwise or concerted pathway.[23,33] For this reason, the quantitative estimate for how much the enzyme−substrate complex lowers the activation barrier for Co−C bond homolysis is a rough approximation. If the reference reaction is based on the rate of homolysis of AdoCbl in solution (10^{-9} s^{-1} at 25 °C), then the $\Delta\Delta G^{\ddagger}$ is ∼73 kJ/mol.[34] If the concerted pathway is invoked, the $\Delta\Delta G^{\ddagger}$ is ∼40 kJ/mol.[22]

Kinetic, structural, and theoretical studies of AdoCbl-dependent isomerases have led to several different proposals for the origin the $\sim 10^{12}$-fold rate acceleration of Co−C bond homolysis.[6,22,29] The strain hypothesis suggests that the enzyme distorts the geometry of the cofactor, leading to substantial weakening of the Co−C bond. Originally, it was proposed that the enzyme compresses the Co−N_{Im} bond, leading to an upward folding of the corrin ring and to strain on the Co−C bond,[35] but this idea has not been supported through resonance Raman spectroscopy[36,37] or the crystal structures of AdoCbl-dependent enzymes.[10,16−18] A modified version of the strain hypothesis centers on the distortion of the Co−C5′−C4′ bond angle that results from the adenosyl group being under increased steric strain in the active site.[29] Two theoretical studies suggested that the catalytic effects originate from specific interactions between residues in the active site and the polar ribose group, but the studies disagree on the degree to which electrostatic versus strain energy weakens the Co−C bond.[22,29] The origin of the discrepancy stems from differences in the computational methods employed by the investigators, as well as difficulties in separating the various energy contributions experimentally.

Orientation of the Adenosyl Group and the Stability of the Co−C Bond. It is evident, especially in the case of OAM, that the adenosyl moiety undergoes a conformational switch upon substrate binding, and this process may place added strain on the Co−C bond. In the edge-on state, the Ado group is in the *syn* orientation with the adenine ring parallel to the B ring of the corrin macrocycle. The OAM Co−C bond is unusually stable in this conformation, as crystal structures show a 2.0 Å distance between the Co and C5′ atoms of the Ado group, revealing an unbroken Co−C bond in a protein structure.[16] Typically, the distance between the two atoms is ≥3 Å in crystal structures of B_{12} enzymes, as the relatively weak organometallic bond is partially or fully reduced by the X-ray beam.[10,18,21]

Insertion of the Ado moiety into the modeled "closed" active site of OAM requires rotation of the adenosyl group to the *anti* conformation about the glycosidic bond, and movement of the adenine ring, such that it is positioned perpendicular to the A pyrrole ring of the corrin macrocycle. This orientation of the Ado group is observed in the structures of MCM and GM.[18,21] Quantum mechanical calculations of the AdoCbl cofactor (including the distally coordinated His) revealed a 21 kJ/mol difference in the bond dissociation energy between the two conformations, indicating that the relative orientation of the Ado moiety with respect to the corrin ring does not significantly influence the lability of the Co−C bond.[15] The orientation of the adenosyl group alone cannot account for the increased stability of the Co−C bond in the resting form of OAM or the activation of this bond during catalysis.

Interestingly, the Co−C bond is mostly cleaved in the crystal structure of lysine 5,6-aminomutase also captured in the edge-on conformation. The lysine 5,6-aminomutase structure shows that the Ado moiety is also in the *syn* conformation about the glycosidic bond.[10] However, unlike in OAM, where the ribose moiety makes polar interactions with the solvent, the corresponding ribose 2′- and 3′-OH groups make electrostatic contacts with the main-chain carbonyls of Glu55 and Asp54 of lysine 5,6-aminomutase. These two residues stem from a six-residue distorted β-hairpin structure that is absent in OAM. Outside of this loop, the structures of OAM and lysine 5,6-aminomutase are structurally conserved. The absence of protein-based polar interactions with the ribose moiety may explain the anomalous stability of the Co−C bond in the OAM crystal structure.

Catalytic Role of Conserved Glutamate. In this work, we have shown that a highly conserved glutamate residue, shown to form polar contacts with the ribose moiety upon substrate binding, plays a major catalytic role in OAM and MCM. Pre-steady-state kinetic analysis of the OAM and MCM mutants revealed no detectable Co−C bond homolysis signal with the natural substrate. For the OAM variants, the rate constants associated with external aldimine formation were similar to that of the native enzyme, suggesting that a reduced rate of catalytic turnover is not attributed to impaired substrate or cofactor binding. The residual activity observed in the OAM and MCM variants indicates that AdoCbl activation is still occurring, but the inability to spectrally observe Co−C bond homolysis suggests that the internal equilibrium constant for the chemical step is shifted in favor of the intact cofactor. Indeed, significantly reduced levels of AdoCbl homolysis observed with DABA further point to an inflated $\Delta G^{\ddagger}$ for radical initiation. Typically, binding of DABA to native OAM converts 40% of the enzyme population to the biradical state.[12]

In the native enzyme, the biradical state persists because abstraction of the C4 hydrogen from the 2,4-diaminobutyryl-PLP external aldimine by the 5′-deoxyadenosyl radical results in an unpaired electron on C4 that is proximal to the Schiff base. Delocalization of the C4 radical through the conjugated π orbital system of the pyridine ring and imine linkage generates a highly stable 2,4-diaminobutyryl-PLP radical that is unable to re-abstract a hydrogen atom from 5′-deoxyadenosine. As a result, the 5′-deoxyadenosyl radical is unable to re-form to

dx.doi.org/10.1021/bi3012719 | Biochemistry 2013, 52, 878−888

recombine with cob(II)alamin, leading to mechanism-based inactivation of the enzyme. In contrast, abstraction of a hydrogen atom from C4 of ornithinyl-PLP results in a highly unstable radical intermediate that undergoes rapid intramolecular isomerization to form product. As a result, free radicals are not observed during steady-state turnover with the physiological substrate.

Of the OAM variants, the E338Q substitution elicited the highest rate of turnover and catalytic efficiency. The observed ~90-fold reduction in activity potentially reflects the weaker nature of dipole−dipole interactions between the Gln side chain and the 2′- and 3′-OH of the ribose compared to dipole−charge interactions present in the native enzyme. Swapping Glu338 for an Asp effectively separates the dipole−charge interaction between the functional groups by an additional ~2 Å. The substantial decrease in catalytic activity (~380-fold) associated with this mutant is attributed to the fact that the strength of the charge−dipole interaction is inversely proportional to r^2, where r is the distance between the two atoms. The low dielectric of the preorganized active site likely further magnifies the energy of interaction between functional groups, accounting for the large differences in activities between wild-type OAM and the E338D and E338Q mutants. It also further suggests that the preorganized active site is relatively ridged and that localized dynamic motion cannot sufficiently compensate for the small increase in charge separation between the protein and the cofactor. Indeed, molecular dynamics simulations of OAM in the edge-on and top-on conformations reveal that the latter catalytically engaged state is significantly less flexible.[15]

The most pronounced decrease in OAM turnover rate occurred with complete removal of the polar side chain in E338A. The fact that catalytic activity is not completely abolished in E338A (turnover and catalytic specificity decreased 670- and 220-fold, respectively) suggests that Glu330 does not solely contribute to Co−C bond rupture. Assuming that Co−C bond homolysis is the rate-limiting step in both wild-type OAM and the E338A mutant, the catalytic contribution of Glu338 is ~16 kJ/mol (assuming $\Delta\Delta G^{\ddagger}$ is 73 kJ/mol). Stopped-flow studies of wild-type OAM reveal that the rate of Co−C bond homolysis is >500 s^{-1}, significantly faster than the turnover rate of 3 s^{-1}.[12] Thus, if we assume that Co−C bond homolysis occurs at a rate of 500 s^{-1} in native OAM but becomes rate-limiting in E338A, with an estimated rate of 4.3×10^{-3} s^{-1}, then it follows that the glutamate side chain is responsible for lowering the $\Delta G^{\ddagger}$ of the Co−C bond homolysis step by ~30 kJ/mol (upper limit). Strikingly, this value is 40 and 75% of the $\Delta\Delta G^{\ddagger}$ estimated for the stepwise and concerted pathways, respectively. The remaining catalytic effect (for surmounting the remaining 10−40 kJ/mol barrier) is possibly distributed among other residues that coordinate to the adenosyl group.

The rate of catalytic turnover for the MCM E392Q and E392D mutants was reduced by 16- and 330-fold, respectively, consistent with the results observed for the corresponding OAM variants. Interestingly, where the glutamate to alanine mutation was the slowest of the OAM variants, MCM E392A retained the highest catalytic activity of the MCM mutants. A possible explanation for this unexpected result is that the short methyl side chain of alanine allows sufficient space for one or more water molecules to enter the active site of MCM and substitute as a polar contact with the hydroxyl groups of the ribose moiety. The importance of the electrostatic interaction with the ribose 2′- and 3′-OH groups is supported by an earlier study that showed that substitution of AdoCbl with 2′,5′-dideoxyadenosylcobalamin resulted in a holo-MCM with only 1−2% activity.[38]

It appears from these data that the conserved Glu significantly reduces the $\Delta G^{\ddagger}$ for Co−C bond homolysis, but the question of whether the side chain weakens the Co−C bond through enforced strain on the ribose (leading to ground-state destabilization) or whether the residue stabilizes the transition state via electrostatic interactions with the ribose remains. Our combined results suggest that the activation barrier to homolysis appears to be dependent on the strength of the electrostatic interaction, given that the strength of the interaction with the 2′- and 3′-OH groups is expected to decrease in a low-dielectric environment with formal charge reduction (E338Q), followed by a 2 Å increase in the length of the charge−dipole interaction (E338D) and then with complete removal of the polar side chain (E338A). Nevertheless, we cannot rule out the possibility that this polar contact places added stain on the Co−C5′−C4′ bond angle.

Activation of the Co−C Bond in the Eliminases. Interestingly, class II eliminases do not appear to have a corresponding Glu coordinated to the adenosyl ribose, suggesting that coordination of protein to the ribose 2′- and 3′-OH groups is not as critical for Co−C bond labilization. This is supported by studies that showed that diol dehydratase retained 31 and 19% activity complexed with 2′-deoxyAdoCbl and 3′-deoxyAdoCbl analogues, respectively.[39] Simulations of EPR spectra of the biradical enzyme reveal that the distance between the cob(II)alamin and the substrate radical is ~11 Å in ethanolamine ammonia lyase[40] and diol dehydratase,[41] whereas the distance between the paramagnetic centers in OAM,[12] MCM,[42] and glutamate mutase[43] is ~6−6.6 Å. The increased distance indicates that Ado$^{\bullet}$ traverses (and likely rotates within) the active site in eliminases. Indeed, high-resolution EPR studies with ethanolamine ammonia lyase shows that the C5′ radical center migrates 5−7 Å to form the substrate-derived radical.[44] Perhaps coordination of the adenosyl moiety to a polar side chain potentially disrupts movement of the radical intermediate along the reaction coordinate.

Concluding Remarks. The work herein highlights the importance of electrostatic interactions between specific active site residues and the adenosyl group to the Co−C bond homolysis event in the class I mutases and class III aminomutases. In particular, a highly conserved glutamate residue potentially accounts for approximately half of the observed decrease in the free energy of activation achieved through binding of the cofactor to these enzymes. Conformational changes upon substrate binding, bringing the glutamate into close contact with the Ado group, afford AdoCbl-dependent enzymes additional control over the generation of reactive radical species during catalysis. Displacement of the glutamate residue from the ribose in the resting state of MCM potentially safeguards against spurious radical generation and enzyme inactivation. This strategy also applies for OAM: rotation of the Rossmann domain away from the active site to form the edge-on conformation likely protects against aberrant Co−C bond homolysis in the absence of substrate. While this mechanism appears to be conserved among the class I and class III enzymes, the class II eliminases, which lack a homologous glutamate residue, likely achieve Co−C bond homolysis through a distinct mechanism.

AUTHOR INFORMATION

Corresponding Author

*Department of Chemistry, University of British Columbia Okanagan, 3333 University Way, Kelowna, BC V1V 1V7, Canada. Phone: (250) 807-8663. Fax: (250) 807-8009. E-mail: kirsten.wolthers@ubc.ca.

Notes

The authors declare no competing financial interest.

ABBREVIATIONS

AdoCbl, adenosylcobalamin; Ado•, 5′-deoxyadenosyl radical; AdoH, 5′-deoxyadenosine; MCM, methylmalonyl-CoA mutase; OAM, ornithine 4,5-aminomutase; PLP, pyridoxal 5′-phosphate; TIM, triosephosphate isomerase; DABA, DL-2,4-diaminobutyric acid; DAP, 2,4-diaminopentanoic acid; DAPDH, 2,4-diaminopentanoic acid dehydrogenase; HEPES, *N*-(2-hydroxyethyl)piperazine-*N*′-2-ethanesulfonic acid; NAD^+, *β*-nicotinamide adenine dinucleotide; EPPS, 4-(2-hydroxyethyl)piperazine-1-propanesulfonic acid; NTA, nitrilotriacetic acid; DTNB, 5,5′-dithiobis(2-nitrobenzoic acid); GDP, guanosine 5′-diphosphate; PDB, Protein Data Bank.

REFERENCES

(1) Brown, K. L. (2005) Chemistry and enzymology of vitamin B-12. *Chem. Rev. 105*, 2075−2149.

(2) Banerjee, R. (2001) Radical peregrinations catalyzed by coenzyme B12-dependent enzymes. *Biochemistry 40*, 6191−6198.

(3) Larsson, K. M., Logan, D. T., and Nordlund, P. (2010) Structural Basis for Adenosylcobalamin Activation in AdoCbl-Dependent Ribonucleotide Reductases. *ACS Chem. Biol. 5*, 933−942.

(4) Banerjee, R. (2003) Radical carbon skeleton rearrangements: Catalysis by coenzyme B12-dependent mutases. *Chem. Rev. 103*, 2083−2094.

(5) Gruber, K., and Kratky, C. (2002) Coenzyme B_{12} dependent glutamate mutase. *Curr. Opin. Chem. Biol. 6*, 598−603.

(6) Toraya, T. (2003) Radical catalysis in coenzyme B12-dependent isomerization (eliminating) reactions. *Chem. Rev. 103*, 2095−2127.

(7) Bandarian, V., and Reed, G. H. (2000) Isotope effects in the transient phases of the reaction catalyzed by ethanolamine ammonia-lyase: Determination of the number of exchangeable hydrogens in the enzyme-cofactor complex. *Biochemistry 39*, 12069−12075.

(8) Chen, H. P., Wu, S. H., Lin, Y. L., Chen, C. M., and Tsay, S. S. (2001) Cloning, sequencing, heterologous expression, purification, and characterization of adenosylcobalamin-dependent D-ornithine aminomutase from *Clostridium sticklandii*. *J. Biol. Chem. 276*, 44744−44750.

(9) Chang, C. H., and Frey, P. A. (2000) Cloning, sequencing, heterologous expression, purification, and characterization of adenosylcobalamin-dependent D-lysine 5,6-aminomutase from *Clostridium sticklandii*. *J. Biol. Chem. 275*, 106−114.

(10) Berkovitch, F., Behshad, E., Tang, K. H., Enns, E. A., Frey, P. A., and Drennan, C. L. (2004) A locking mechanism preventing radical damage in the absence of substrate, as revealed by the X-ray structure of lysine 5,6-aminomutase. *Proc. Natl. Acad. Sci. U.S.A. 101*, 15870−15875.

(11) Mancia, F., and Evans, P. R. (1998) Conformational changes on substrate binding to methylmalonyl CoA mutase and new insights into the free radical mechanism. *Structure 6*, 711−720.

(12) Wolthers, K. R., Rigby, S. E., and Scrutton, N. S. (2008) Mechanism of radical-based catalysis in the reaction catalyzed by adenosylcobalamin-dependent ornithine 4,5-aminomutase. *J. Biol. Chem. 283*, 34615−34625.

(13) Maity, A. N., Hsieh, C. P., Huang, M. H., Chen, Y. H., Tang, K. H., Behshad, E., Frey, P. A., and Ke, S. C. (2009) Evidence for conformational movement and radical mechanism in the reaction of 4-thia-L-lysine with lysine 5,6-aminomutase. *J. Phys. Chem. B 113*, 12161−12163.

(14) Shibata, N., Masuda, J., Morimoto, Y., Yasuoka, N., and Toraya, T. (2002) Substrate-induced conformational change of a coenzyme B12-dependent enzyme: Crystal structure of the substrate-free form of diol dehydratase. *Biochemistry 41*, 12607−12617.

(15) Pang, J., Li, X., Morokuma, K., Scrutton, N. S., and Sutcliffe, M. J. (2012) Large-scale domain conformational change is coupled to the activation of the Co-C bond in the B12-dependent enzyme ornithine 4,5-aminomutase: A computational study. *J. Am. Chem. Soc. 134*, 2367−2377.

(16) Wolthers, K. R., Levy, C., Scrutton, N. S., and Leys, D. (2010) Large-scale domain dynamics and adenosylcobalamin reorientation orchestrate radical catalysis in ornithine 4,5-aminomutase. *J. Biol. Chem. 285*, 13942−13950.

(17) Mancia, F., Keep, N. H., Nakagawa, A., Leadlay, P. F., McSweeney, S., Rasmussen, B., Bosecke, P., Diat, O., and Evans, P. R. (1996) How coenzyme B12 radicals are generated: The crystal structure of methylmalonyl-coenzyme A mutase at 2 Å resolution. *Structure 4*, 339−350.

(18) Reitzer, R., Gruber, K., Jogl, G., Wagner, U. G., Bothe, H., Buckel, W., and Kratky, C. (1999) Glutamate mutase from *Clostridium cochlearium*: The structure of a coenzyme B12-dependent enzyme provides new mechanistic insights. *Structure 7*, 891−902.

(19) Gruber, K., Reitzer, R., and Kratky, C. (2001) Radical Shuttling in a Protein: Ribose Pseudorotation Controls Alkyl-Radical Transfer in the Coenzyme B_{12} Dependent Enzyme Glutamate Mutase. *Angew. Chem., Int. Ed. 40*, 3377−3380.

(20) Ludwig, M. L., and Matthews, R. G. (1997) Structure-based perspectives on B12-dependent enzymes. *Annu. Rev. Biochem. 66*, 269−313.

(21) Froese, D. S., Kochan, G., Muniz, J. R., Wu, X., Gileadi, C., Ugochukwu, E., Krysztofinska, E., Gravel, R. A., Oppermann, U., and Yue, W. W. (2010) Structures of the human GTPase MMAA and vitamin B12-dependent methylmalonyl-CoA mutase and insight into their complex formation. *J. Biol. Chem. 285*, 38204−38213.

(22) Sharma, P. K., Chu, Z. T., Olsson, M. H., and Warshel, A. (2007) A new paradigm for electrostatic catalysis of radical reactions in vitamin B12 enzymes. *Proc. Natl. Acad. Sci. U.S.A. 104*, 9661−9666.

(23) Bucher, D., Sandala, G. M., Durbeej, B., Radom, L., and Smith, D. M. (2012) The elusive 5′-deoxyadenosyl radical in coenzyme-B12-mediated reactions. *J. Am. Chem. Soc. 134*, 1591−1599.

(24) Makins, C., Miros, F. N., Scrutton, N. S., and Wolthers, K. R. (2012) Role of histidine 225 in adenosylcobalamin-dependent ornithine 4,5-aminomutase. *Bioorg. Chem. 40*, 39−47.

(25) Taoka, S., Padmakumar, R., Lai, M. T., Liu, H. W., and Banerjee, R. (1994) Inhibition of the human methylmalonyl-CoA mutase by various CoA-esters. *J. Biol. Chem. 269*, 31630−31634.

(26) McKie, N., Keep, N. H., Patchett, M. L., and Leadlay, P. F. (1990) Adenosylcobalamin-dependent methylmalonyl-CoA mutase from *Propionibacterium shermanii*. Active holoenzyme produced from *Escherichia coli*. *Biochem. J. 269*, 293−298.

(27) Padmakumar, R., Padmakumar, R., and Banerjee, R. (1997) Evidence that cobalt-carbon bond homolysis is coupled to hydrogen atom abstraction from substrate in methylmalonyl-CoA mutase. *Biochemistry 36*, 3713−3718.

(28) Chowdhury, S., and Banerjee, R. (1999) Role of the dimethylbenzimidazole tail in the reaction catalyzed by coenzyme B12-dependent methylmalonyl-CoA mutase. *Biochemistry 38*, 15287−15294.

(29) Jensen, K. P., and Ryde, U. (2005) How the Co-C bond is cleaved in coenzyme B12 enzymes: A theoretical study. *J. Am. Chem. Soc. 127*, 9117−9128.

(30) Durbeej, B., Sandala, G. M., Bucher, D., Smith, D. M., and Radom, L. (2009) On the importance of ribose orientation in the substrate activation of the coenzyme B12-dependent mutases. *Eur. J. Chem. 15*, 8578−8585.

(31) Marsh, E. N., and Melendez, G. D. (2012) Adenosylcobalamin enzymes: Theory and experiment begin to converge. *Biochim. Biophys. Acta 1824*, 1154−1164.

(32) Marsh, E. N., and Ballou, D. P. (1998) Coupling of cobalt-carbon bond homolysis and hydrogen atom abstraction in adenosylcobalamin-dependent glutamate mutase. *Biochemistry 37*, 11864−11872.
(33) Kozlowski, P. M., Kamachi, T., Toraya, T., and Yoshizawa, K. (2007) Does Cob(II)alamin act as a conductor in coenzyme B12 dependent mutases? *Angew. Chem., Int. Ed. 46*, 980−983.
(34) Finke, R. G., and Martin, B. D. (1990) Coenzyme AdoB12 vs AdoB12-homolytic Co-C cleavage following electron transfer: A rate enhancement $\geq 10^{12}$. *J. Inorg. Biochem. 40*, 19−22.
(35) Halpern, J. (1985) Mechanisms of coenzyme B12-dependent rearrangements. *Science 227*, 869−875.
(36) Dong, S. L., Padmakumar, R., Banerjee, R., and Spiro, T. G. (1999) Co-C bond activation in B-12-dependent enzymes: Cryogenic resonance Raman studies of methylmalonyl-coenzyme A mutase. *J. Am. Chem. Soc. 121*, 7063−7070.
(37) Huhta, M. S., Chen, H. P., Hemann, C., Hille, C. R., and Marsh, E. N. (2001) Protein-coenzyme interactions in adenosylcobalamin-dependent glutamate mutase. *Biochem. J. 355*, 131−137.
(38) Calafat, A. M., Taoka, S., Puckett, J. M., Jr., Semerad, C., Yan, H., Luo, L., Chen, H., Banerjee, R., and Marzilli, L. G. (1995) Structural and electronic similarity but functional difference in methylmalonyl-CoA mutase between coenzyme B12 and the analog 2′,5′-dideoxyadenosylcobalamin. *Biochemistry 34*, 14125−14130.
(39) Toraya, T., and Fukui, S. (1977) Immunochemical evidence for the difference between coenzyme-B12-dependent diol dehydratase and glycerol dehydratase. *Eur. J. Biochem. 76*, 285−289.
(40) Bandarian, V., and Reed, G. H. (2002) Analysis of the electron paramagnetic resonance spectrum of a radical intermediate in the coenzyme B_{12}-dependent ethanolamine ammonia-lyase catalyzed reaction of S-2-aminopropanol. *Biochemistry 41*, 8580−8588.
(41) Abend, A., Bandarian, V., Reed, G. H., and Frey, P. A. (2000) Identification of cis-ethanesemidione as the organic radical derived from glycolaldehyde in the suicide inactivation of dioldehydrase and of ethanolamine ammonia-lyase. *Biochemistry 39*, 6250−6257.
(42) Mansoorabadi, S. O., Magnusson, O. T., Poyner, R. R., Frey, P. A., and Reed, G. H. (2006) Analysis of the cob(II)alamin-5′-deoxy-3′,4′-anhydroadenosyl radical triplet spin system in the active site of diol dehydrase. *Biochemistry 45*, 14362−14370.
(43) Bothe, H., Darley, D. J., Albracht, S. P., Gerfen, G. J., Golding, B. T., and Buckel, W. (1998) Identification of the 4-glutamyl radical as an intermediate in the carbon skeleton rearrangement catalyzed by coenzyme B12-dependent glutamate mutase from *Clostridium cochlearium*. *Biochemistry 37*, 4105−4113.
(44) Warncke, K., and Utada, A. S. (2001) Interaction of the substrate radical and the 5′-deoxyadenosine-5′-methyl group in vitamin B_{12} coenzyme-dependent ethanolamine deaminase. *J. Am. Chem. Soc. 123*, 8564−8572.